Advanced Nano Research
Volume 4, Issue 1, pp. 1-9, 2021
DOI: https://doi.org/10.21467/anr.4.1.1-9
ISSN: 2581-5164
RESEARCH ARTICLE

Excitonic States and Related Optical Susceptibility in InN/AlN Quantum Well Under the Effects of the Well Size and Impurity Position

Fathallah Jabouti[1], Haddou El Ghazi[1,2,*], Redouane En-nadir[1*], Izeddine Zorkani[1], Anouar Jorio[1]

[1]Sidi Mohammed Ben Abdellah University, Fes, Morocco,
[2]ENSAM Laboratory, Hassan II University, Casablanca, Morocco

[*]Corresponding author email: hadghazi@gmail.com; redouane.en-nadir@usmba.ac.ma

Received: 10 May 2021 / Accepted: 09 August 2021 / Published: 01 September 2021

ABSTRACT

Based on the finite difference method, linear optical susceptibility, photoluminescence peak and binding energies of three first states of an exciton trapped by a positive charge donor-impurity (D^+, X) confined in InN/AlN quantum well are investigated in terms of well size and impurity position. The electron, heavy hole free and bound excitons allowed eigen-values and corresponding eigen-functions are obtained numerically by solving one-dimensional time-independent Schrödinger equation. Within the parabolic band and effective mass approximations, the calculations are made considering the coupling of the electron in the n-th conduction subband and the heavy hole in the m-th valence subband under the impacts of the well size and impurity position. The obtained results show clearly that the energy, binding energy and photoluminescence peak energy show a decreasing behavior according to well size for both free and bound cases. Moreover, the optical susceptibility associated to exciton transition is strongly red-shift (blue-shifted) with enhancing the well size (impurity position).

Keywords: Quantum well, Exciton-states, Binding energy, Susceptibility.

1 Introduction

In the few last decades, hetero-structures based semiconductor materials have drawn much attention owing to diverse electronic and optical applications. Due to noteworthy flexibility of their properties and resulted radiative characteristics such as exciton-light coupling, the most studied hetero-structures is the lattice matched GaAs-based ones with single quantum well (QW). Fundamental properties of excitons and their light-coupling were used to understand the reflectance spectra, namely, the energy resonance and optical response shape. The exciton resonances energies as well as the oscillator strengths and the radiative decay are reported. With the development of micro-cavities, such properties have been of momentous interest in QW hetero-structures[1]–[6]. To understand electronic and optical properties of more complicated systems as asymmetric QW, coupled double QWs, multiple coupled QWs and low-dimensional system under different external perturbations[7]–[20] , a basic comprehensive knowledge of exciton states in rectangular QW becomes necessary. Added to geometric confinement, the Coulomb interaction between electron and hole ground and excited states leads to large exciton binding energy and a strong optical response for the exciton resonance. This is considered as a key parameter to interpret the experimental photoluminescence (PL) and reflectance spectra [21]–[23]. Recently, this latter is one of the most techniques used with great accuracy to identify exciton states as well as their radiative and non-radiative broadenings compared to the PL spectra.

To describe the exciton states in QW, several papers are reported based on the time-independent Schrödinger equation solving using different approaches such: the perturbative method[24], the Ritz-variational method[12]–[14], the shooting method[25] and the Hartree formalism with a recently developed numerical method (Potential Morphing Method). Recently, Belov[26] has used the finite difference method which allows him to obtain exciton states and binding energies for a wide domain of well widths considering the discontinuities of the material parameters at the square QW interfaces. Such numerical method does not rely to a prescribed form of the trial functions, which allow one to obtain the exciton electronic, and optical characteristics.

With the motivation of all such attractive properties of QW systems, the present paper is dedicated to evolve the influence the size and impurity position on the free and bound excitons binding energies and intersubband exciton related linear optical susceptibility in rectangular InN/AlN QW.

2 Theoretical framework

We consider the heavy free and bound excitons (D^+, X) confined in InN/AlN QW hetero-structure as shown in Fig. 1. The particle's Hamiltonian within the framework of effective mass and parabolic approximations can be described as following:

$$H_x = H_e + H_h + H_{e-h} \qquad (1)$$

The first and the second terms are the electron and hole Hamiltonian operators confined along the z-direction in the presence of the positive charge donor-impurity, given as:

$$H_{e,h} = -\frac{\hbar^2}{2}\frac{d}{dz}\left[\frac{1}{m^*(z)}\frac{d}{dz}\right] \mp \frac{\alpha e^2}{4\pi\varepsilon_0\varepsilon^*(z)|\vec{r}_{e,h}-\vec{r}_0|} + V_{e,h}(z) \qquad (2)$$

Where, the signs (-) and (+) correspond respectively to the electron and hole, $V_{e,h}(z)$ is the band offset potential barrier, $\alpha(=0;1)$ corresponds to the free and bound exciton particles respectively, $m^*(z)$ and $\varepsilon^*(z)$ are the z-dependent effective mass and relative dielectric constant.

The third term in Eq. (1) describes the electron-heavy hole interaction. It is expressed as following:

$$H_{e-h} = -\frac{\hbar^2}{2\mu_\perp}\vec{\nabla}_\perp^2 - \frac{e^2}{4\pi\varepsilon_0\varepsilon^*(z)|\vec{r}_e-\vec{r}_h|} \qquad (3)$$

Where, $\mu_\perp$ and $\nabla_\perp$ are respectively the reduced effective mass and the perpendicular 2D Laplacian operator.

Based on the finite difference method, the electron, hole and exciton energies are obtained numerically. We have restricted ourselves to investigate ground and first excited states for electron and heavy hole on the one hand and the ground and two first excited states of the exciton. Considering the coupling of the electron in the n-th conduction subband and the heavy hole in the m-th valence subband, the exciton states ($i \equiv 0,1,2$) bending energies are expressed as following:

$$E_{b,i}^{n,m} = E_e^n + E_{hh}^m - E_X^i \qquad (4)$$

Once obtained the particle energies, it becomes easy to calculate the position of different states-dependent photoluminescence peak given by:

$$E_{PL,i}^{n,m} = E_e^n + E_{hh}^m + E_g^{InN} + E_X^i \qquad (5)$$

Where, E_g^{InN} is the InN band gap energy at room temperature.

The oscillator strength and the linear complex optical susceptibility are given as following:

$$\begin{cases} \mathcal{P}_{if} = \frac{2m^*}{\hbar^2}\Delta E_{if}\left|M_{if}\right|^2 \\ \bar{\chi}(w) = \frac{\mathcal{P}_{if}}{\left(\hbar w - E_{PL,i\to f}^{n,m} - j\,\hbar\Gamma_{i\to f}\right)} \end{cases} \qquad (6)$$

Note that, $M_{if}\left(=\langle\Psi_f|ez|\Psi_i\rangle\right)$ is the electric dipole matrix element of the transition from initial to final exciton states in QW, $\Delta E_{if}\left(=E_f - E_i\right)$ denotes their energy difference, $\Gamma_{fi} = \frac{1}{\tau_{fi}}\ (=5\times10^{12}\mathrm{s}^{-1})$ is the relaxation time between them and $j\ (j^2=-1)$ is the complex number.

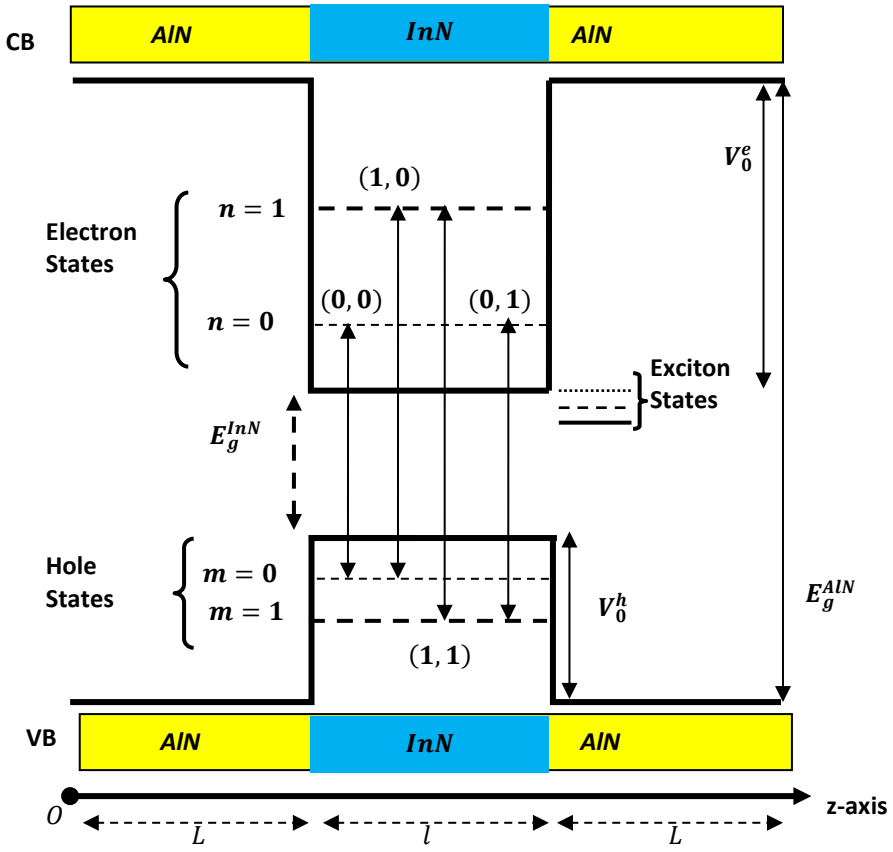

Figure 1: *Schematic diagram of the studied InN/AlN hetero-structure.*

The parameters that we have used in our calculations are the same as those of previous work [27].

3 Results and discussion

We have studied the bending energies and the linear optical susceptibility related to three different exciton states coupling to two first electron and heavy hole states. Due to a large band offset between InN $\left(E_g^{InN} = 0.8\,eV\right)$ and AlN $\left(E_g^{AlN} = 6.2\,eV\right)$ equals to $4.32\,eV$, we restricted ourselves to an infinite potential case which remains a good approximation describing the particle wave-function in the well. We considered free and bound excitons and studied the behavior of both cases versus the structure size.

Firstly, let us discuss the impurity's effects on the electron and hole energies as shown in Figure 2. Panels (a) and (b) show that the energies decrease according to the well width at room temperature for both cases. Regardless the state, it is obvious that the presence of the impurity ($\alpha = 1$) induces a significant shrink (enhancement) for the electron (hole) energy as expected from Eq. (2). This effect is more remarkable for large well than for thin one. Panel (c) shows a similar behavior for the four first exciton state energies. In addition, we can see that the free exciton state energies are lower than those of bound one for all structure size.

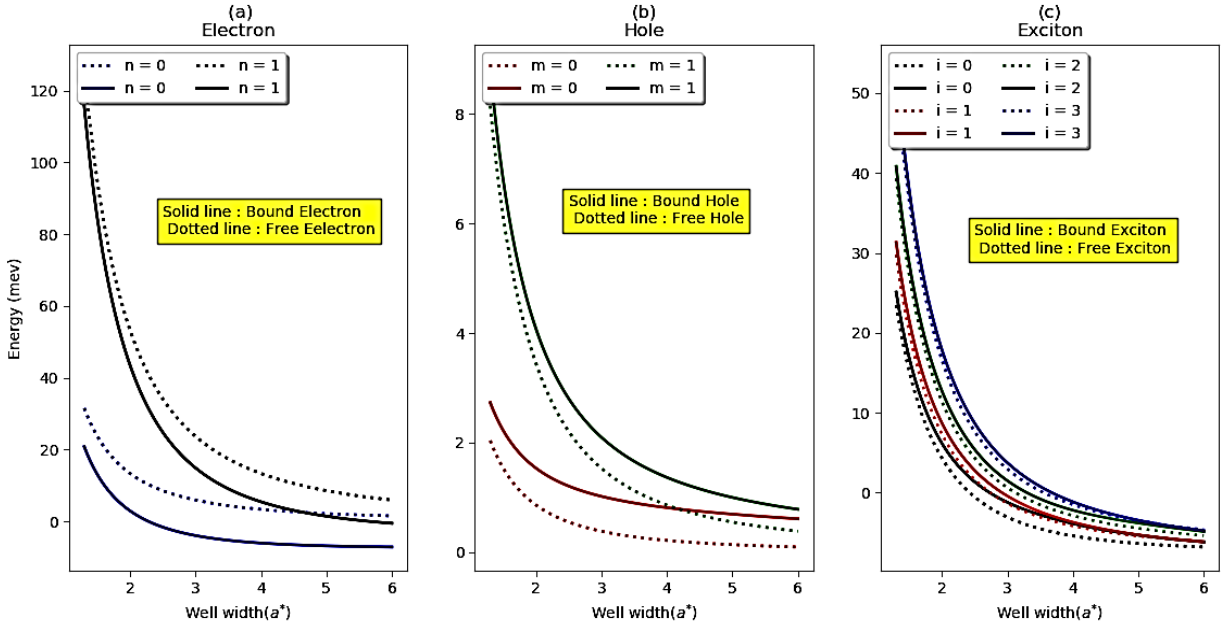

Figure 2: *(Color online) Particle energy versus InN/AlN sturture size at room temperature. Panel (a) and (b): two electron and heavy-hole first states, Panel (c): the four first free and bound exciton states.*

Fig. (3) illustrates the exciton binding energy versus the well width for three first states considering the impurity influences. The solid line indicates the values of bound exciton binding energy while the dotted line designates a free exciton one. A similar decrease is revealed with increasing the well width independently of states which is due to the widening of confinement region.

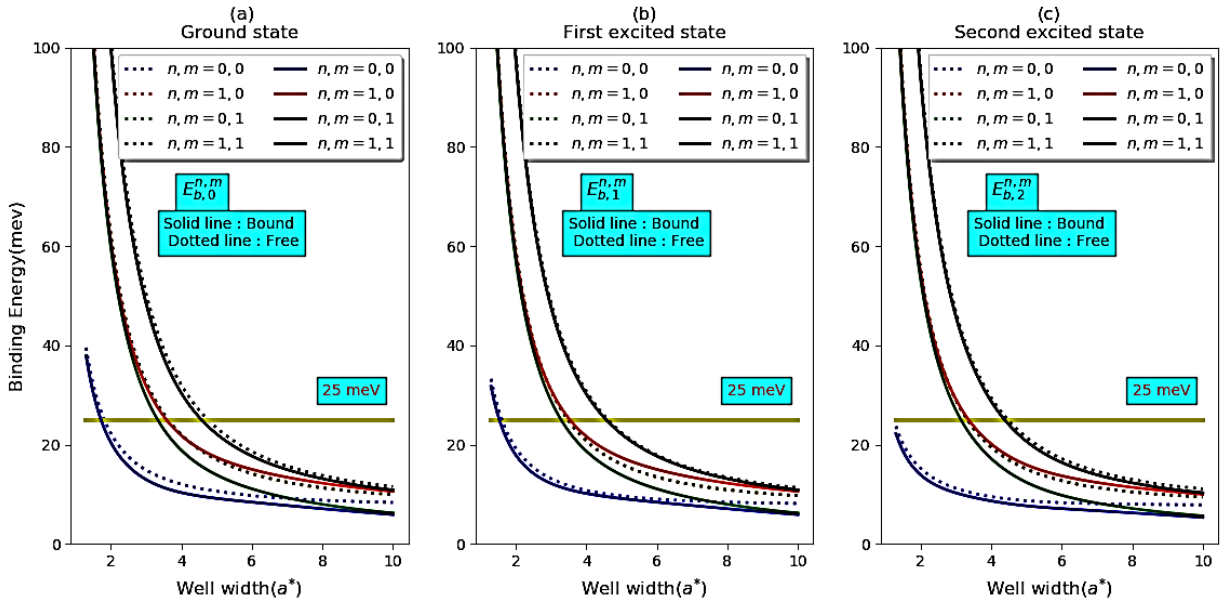

Figure 3: *(Color online) The exciton binding energy as a function of the well width at room temperature coupling to ground and first excited electron and heavy-hole states. Panel (a): ground exciton state, Panels (b) and (c) :first and second excited exciton states.*

It is observed that the inclusion of the impurity enhances the exciton binding energy in all cases. As long as the well widens the exciton binding energies become tighter and converges to the bulk behavior. The horizontal line located at 25mev designates the exciton thermodynamic stability limit at 300K. It

appears that the exciton states are thermodynamically stable at room temperature for well width smaller than a critical value. For instance, this latter is equal to 1.68, 1.51 and 1.24 for $(n,m) = (0,0)$ while it is equal to 4.57, 4.54 and 4.45 for $(n,m) = (1,1)$ for the ground, first and second excited exciton states. Incidentally, it is important to mention that the InN bulk ground state binding energy is about 15 meV which shows that it is unstable at 300K contrary to the InN QW in which the stability depends on the size. Moreover, it is clearly seen that the free exciton binding energy is slightly greater than the bound exciton case for all states. This implies that with the impurity, the hole binding energy enhancement masks the electron drop one.

In order to show more the effects of the impurity on the free and bound excitons binding energies, we have presented in Fig. 4 the difference $\Delta E_{b,i}^{n,m}\left(= E_{b,i}^{n,m}(Free) - E_{b,i}^{n,m}(Bound)\right)$. It is observed that the QW width has a great influence since the curvature is not monotonic. For a critical value of the well width, this difference reaches a maximum for all transitions. It is clear that the $(n,m) = (1,0)$ and (1,1) transition energies tend to the same limit while $(n,m) = (0,0)$ and $(0,1)$ converge to other limit as the well size increases.

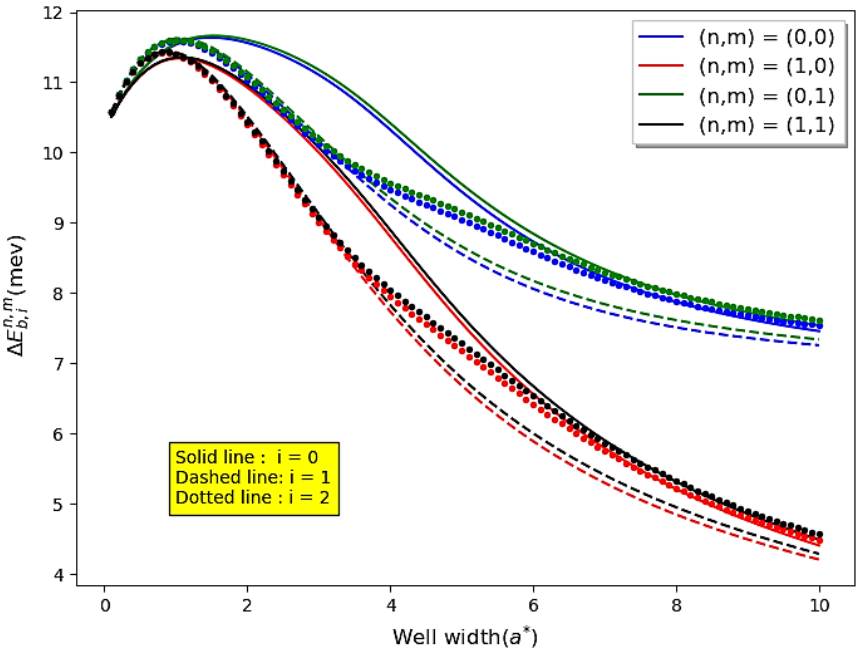

Figure 4: *(Color online) The exciton binding energy difference as a function of the well width at room temperature.*

With obtaining the electron, heavy hole and exciton energies one can compute the photoluminescence energy (PLE) versus the well width. The PLE (interband transition) is depicted on Figure 5 as a function of the well size. It is shown that the transition energy (PLE) decreases monotonically with increasing the well size as expected. The physical reason is that as the QW width increases, the energy levels of both electron and hole are lowered (Fig. 2) which is due to the quantum confinement size. It is also observed that the inclusion of the impurity effects leads to the drop of the PLE, i.e., the free transition energy is significantly greater than the bound one for all transitions in particularly for large well. Such behavior can be assigned to the fact that the electron-impurity Coulomb interaction is more significant than the hole-impurity one. For thin well, the free and bound exciton PLE converge to the same results.

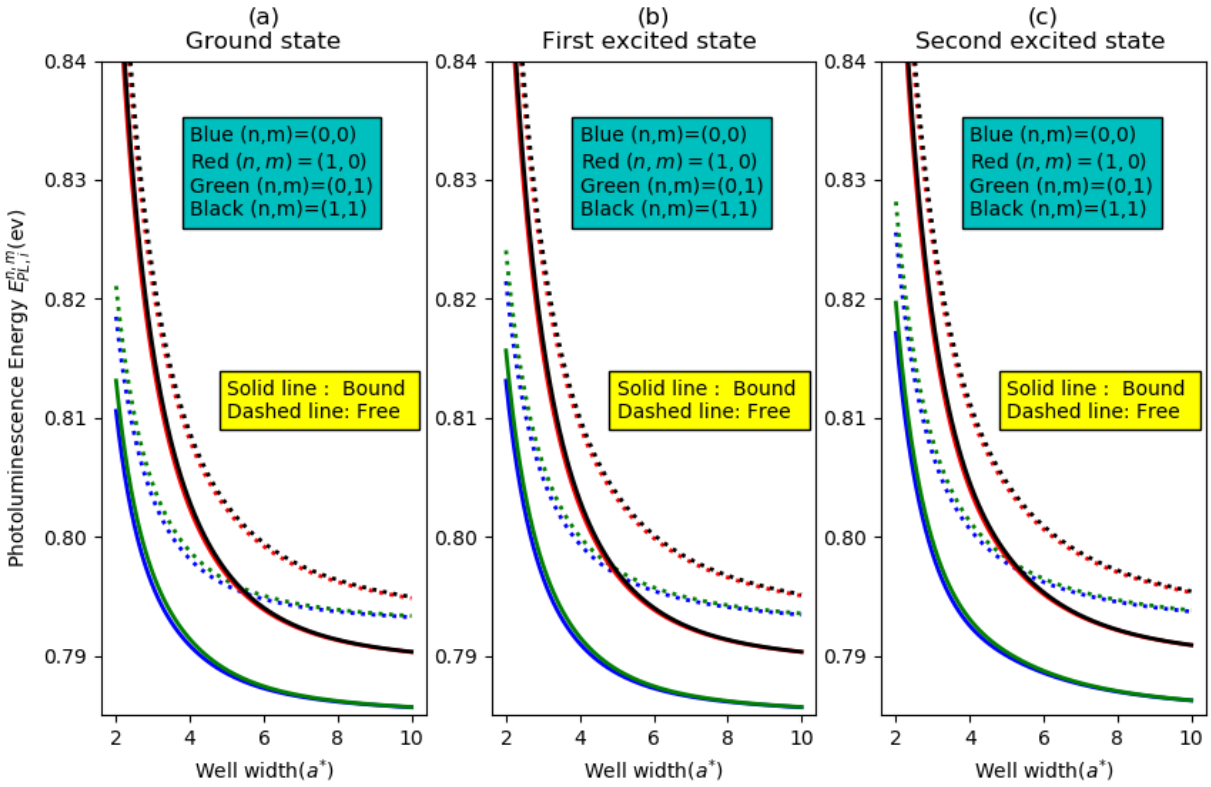

Figure 5: *(Color online) The exciton photoluminescence energy according the well width at room temperature coupling to ground and first excited electron and heavy-hole states. Panel (a): ground exciton state, Panels (b) and (c) : first and second excited exciton states.*

In order to further investigate the quantum size, the presence of the impurity and its position effects on the InN/AlN QW optical properties, we present on fig. 6 the imaginary part of linear susceptibility related to interband exciton transitions versus the photon energy at room temperature. Panels (a), (b), (c) and (d) depict the size effect for on-center impurity while panels (c), (d), (e) and (f) illustrate the impurity position influences for $l = 4$. With regard to this figure, one readily notices that their variations are not monotonic but present a maximum for photon energy's critical value. All panels reveal clearly that the imaginary part increases with increasing the photon energy for reaching its maximum and then began to decreases. It should be notice that the maximum is obtained for the photon energy equal to $E_e^n + E_{hh}^m + E_g^{InN} + E_X^{i\to f}$. For $(e_{0,}, h_1)$, it is equal respectively to 807.12, 808.81 and 811.34 meV for different exciton transitions $(i, f) = (0,1)$, $(0,2)$ and $(1,2)$. It is obvious that with increasing the well width a significant redshift is revealed for all exciton transitions. For instance, a redshift of about 11.981, 14.862 and 12.567 meV is obtained for ground-first excited, ground-second excited and first-second excited states optical transition for (e_0, h_1). On the other hand, with displacing the impurity from structure center to the band edge an important blueshift is illustrated for all exciton transitions. For example, a blue shift of 3.734 meV is revealed first-second excited states transition coupled to electron in the ground state and the hole in the first excited state, (e_0, h_1).

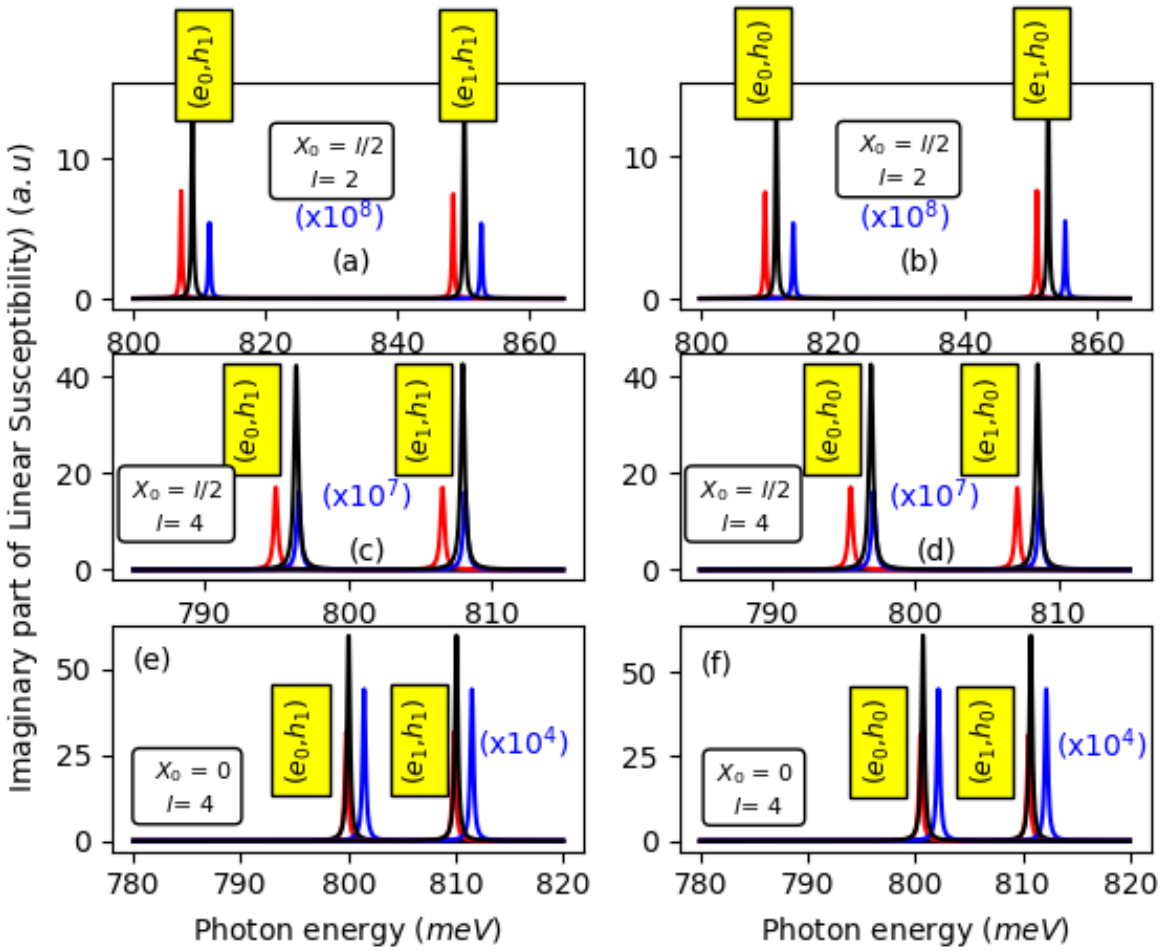

Figure 6: *(Color online) The bound exciton-related imaginary part of the susceptibility as a function of the photon energy at room temperature. Red line: ground-first excited states transition, blue line (Multiplied for more visibility): ground-second excited states transition and black line: first-second excited states transition.*

Figure 7 illustrates the variation of the real part of the linear susceptibility according to the photon energy under the impacts of size and the impurity's position. Compared to the imaginary one, different behaviors are obtained. At the beginning, it increases steadily to reach its maximum with increasing the photon energy. Then, it decreases quickly for reaching its minimum and increases as long as the photon energy $(\hbar w)$ augments. It should be notice that the extremum are located at $E_e^n + E_{hh}^m + E_g^{InN} + E_X^{i\to f} \pm \hbar\Gamma_{i\to f}$. The spectral range between the minimum and the maximum corresponds to the absorption band characterized by a strong absorption phenomenon which is in good agreement with the above results. Compared to the imaginary one, a similar behavior (Blue and red shifts) is obtained under the effects of well width and impurity position for real part.

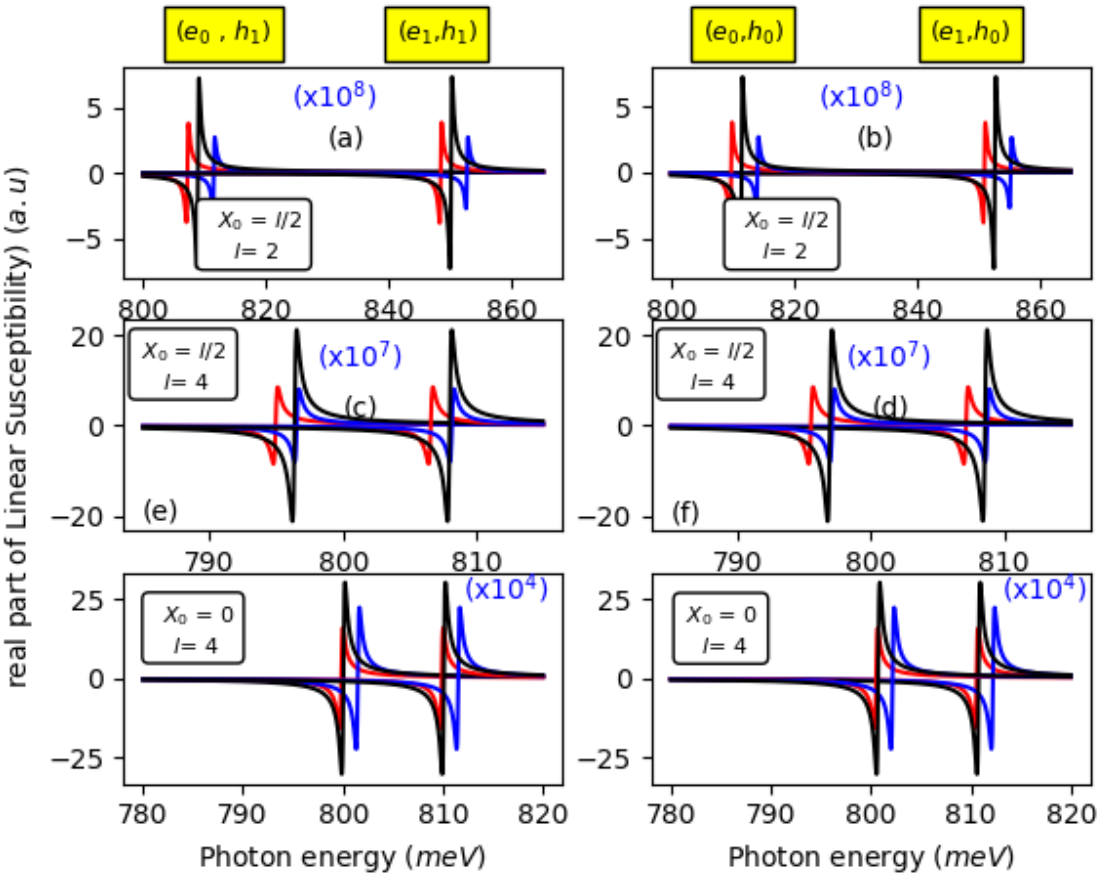

Figure 7: *(Color online) The bound exciton-related imaginary part of the susceptibility as a function of the photon energy at room temperature. Red line: ground-first excited states transition, blue line (Multiplied for more visibility): ground-second excited states transition and black line: first-second excited states transition.*

Finally, our results are generally in good conformity compared with the finding results in the literature concerning different materials and well shapes [28],[29]. Some discrepancies remain due to the fact that in our calculations we have taken into account the presence of the impurity (Bound exciton) neglected generally in the literature.

4 Conclusion

In summary, we have investigated theoretically the ground, first and second excited states exciton (D^+, X) binding energies, photoluminescence energy and linear optical susceptibility taking into account of the electron in the n-th conduction subband and the heavy hole in the m-th valence subband coupling. Numerical results show that the free and bound exciton binding energies and exciton related-PLE are highly dependent on the well size and impurity position showing a significant shrink according to the well size. Moreover, it is obtained that the inclusion of the Coulomb interaction leads to the drop of the binding energy for all states. Additionally, both linear optical susceptibility counterparts reveal that with increasing the well size and/or the displacement of the impurity from the band edge toward the structure center induces a noteworthy redshift.

5 Competing Interests

The authors declared that they do not have any conflict of interest in this publication.

How to Cite this Article:

F. Jabouti, H. El Ghazi, R. En-nadir, I. Zorkani, and A. Jorio, "Excitonic States and Related Optical Susceptibility in InN/AlN Quantum Well Under the Effects of the Well Size and Impurity Position", *Adv. Nan. Res.*, vol. 4, no. 1, pp. 1–9, 2021. https://doi.org/10.21467/anr.4.1.1-9

References

[1] F. Schweiner, J. Main, and G. Wunner, 'Linewidths in excitonic absorption spectra of cuprous oxide', *Phys. Rev. B*, vol. 93, no. 8, p. 085203, 2016.
[2] M. Van der Donck, M. Zarenia, and F. M. Peeters, 'Excitons, trions, and biexcitons in transition-metal dichalcogenides: magnetic-field dependence', *Phys. Rev. B*, vol. 97, no. 19, p. 195408, 2018.
[3] T. Kazimierczuk, D. Fröhlich, S. Scheel, H. Stolz, and M. Bayer, 'Giant Rydberg excitons in the copper oxide Cu 2 O', *Nature*, vol. 514, no. 7522, pp. 343–347, 2014.
[4] A. Alvermann and H. Fehske, 'Exciton mass and exciton spectrum in the cuprous oxide', *J. Phys. B At. Mol. Opt. Phys.*, vol. 51, no. 4, p. 044001, 2018.
[5] F. Schöne *et al.*, 'Deviations of the exciton level spectrum in Cu 2 O from the hydrogen series', *Phys. Rev. B*, vol. 93, no. 7, p. 075203, 2016.
[6] G. Wang *et al.*, 'Colloquium: Excitons in atomically thin transition metal dichalcogenides', *Rev. Mod. Phys.*, vol. 90, no. 2, p. 021001, 2018.
[7] P. S. Grigoryev *et al.*, 'Excitons in asymmetric quantum wells', *Superlattices Microstruct.*, vol. 97, pp. 452–462, 2016.
[8] B. Laikhtman, 'Direct and indirect exciton mixture in double quantum wells', *EPL Europhys. Lett.*, vol. 123, no. 6, p. 67001, 2018.
[9] E. A. Koval and O. A. Koval, 'Excited states of two-dimensional hydrogen atom in tilted magnetic field: Quantum chaos', *Phys. E Low-Dimens. Syst. Nanostructures*, vol. 93, pp. 160–166, 2017.
[10] R. P. Seisyan, A. V. Kavokin, K. Moumanis, and M. E. Sasin, 'Effect of a Coulomb well in (In, Ga) As/GaAs quantum wells', *Phys. Solid State*, vol. 59, no. 6, pp. 1154–1170, 2017.
[11] P. S. Grigoryev *et al.*, 'Exciton-light coupling in (In, Ga) As/GaAs quantum wells in a longitudinal magnetic field', *Phys. Rev. B*, vol. 96, no. 15, p. 155404, 2017.
[12] R. Harris, J. Terblans, and H. Swart, 'Exciton binding energy in an infinite potential semiconductor quantum well–wire heterostructure', *Superlattices Microstruct.*, vol. 86, pp. 456–466, 2015.
[13] S. Wu, L. Cheng, and Q. Wang, 'Excitonic effects and related properties in semiconductor nanostructures: roles of size and dimensionality', *Mater. Res. Express*, vol. 4, no. 8, p. 085017, 2017.
[14] M. Y. Gubin, A. V. Shesterikov, S. N. Karpov, and A. V. Prokhorov, 'Entangled plasmon generation in nonlinear spaser system under the action of external magnetic field', *Phys. Rev. B*, vol. 97, no. 8, p. 085431, 2018.
[15] Y. Z. Han and C. S. Liu, 'The nontrivial topological phases of indirect excitons in semiconductor coupled quantum wells', *Phys. E Low-Dimens. Syst. Nanostructures*, vol. 108, pp. 116–122, 2019.
[16] V. A. Stephanovich, E. Y. Sherman, N. T. Zinner, and O. V. Marchukov, 'Energy-level repulsion by spin-orbit coupling in two-dimensional Rydberg excitons', *Phys. Rev. B*, vol. 97, no. 20, p. 205407, 2018.
[17] C. Abbas *et al.*, 'Spin relaxation of indirect excitons in asymmetric coupled quantum wells', *Superlattices Microstruct.*, vol. 122, pp. 643–649, 2018.
[18] S. I. Tsintzos *et al.*, 'Electrical tuning of nonlinearities in exciton-polariton condensates', *Phys. Rev. Lett.*, vol. 121, no. 3, p. 037401, 2018.
[19] M. D. Fraser, 'Coherent exciton-polariton devices', *Semicond. Sci. Technol.*, vol. 32, no. 9, p. 093003, 2017.
[20] M. Combescot, R. Combescot, and F. Dubin, 'Bose–Einstein condensation and indirect excitons: a review', *Rep. Prog. Phys.*, vol. 80, no. 6, p. 066501, 2017.
[21] A. S. Bolshakov *et al.*, 'Room temperature exciton-polariton resonant reflection and suppressed absorption in periodic systems of InGaN quantum wells', *J. Appl. Phys.*, vol. 121, no. 13, p. 133101, 2017.
[22] S. Gies, B. Holz, C. Fuchs, W. Stolz, and W. Heimbrodt, 'Recombination dynamics of type-II excitons in (Ga, In) As/GaAs/Ga (As, Sb) heterostructures', *Nanotechnology*, vol. 28, no. 2, p. 025701, 2016.
[23] Y. Chen *et al.*, 'Resonant optical properties of AlGaAs/GaAs multiple-quantum-well based Bragg structure at the second quantum state', *J. Appl. Phys.*, vol. 121, no. 10, p. 103101, 2017.
[24] A. J. Peter and C. W. Lee, 'Binding energy and radiative lifetime of an exciton in a type-II quantum well', *Phys. Scr.*, vol. 85, no. 1, p. 015704, 2011.
[25] J. Wilkes and E. A. Muljarov, 'Excitons and polaritons in planar heterostructures in external electric and magnetic fields: A multi-sub-level approach', *Superlattices Microstruct.*, vol. 108, pp. 32–41, 2017.
[26] P. A. Belov, 'Energy spectrum of excitons in square quantum wells', *Phys. E Low-Dimens. Syst. Nanostructures*, vol. 112, pp. 96–108, 2019.
[27] H. El Ghazi and A. J. Peter, 'Built-in electric field effect on optical absorption spectra of strained (In, Ga) N–GaN nanostructures', *Phys. B Condens. Matter*, vol. 470, pp. 64–68, 2015.